

## Spectroscopic Evidence for Multiple Order Parameter Components in the Heavy Fermion Superconductor CeCoIn<sub>5</sub>

P. M. C. Rourke,<sup>1</sup> M. A. Tanatar,<sup>1,\*</sup> C. S. Turel,<sup>1</sup> J. Berdeklis,<sup>1</sup> C. Petrovic,<sup>2</sup> and J. Y. T. Wei<sup>1</sup>

<sup>1</sup>*Department of Physics, University of Toronto, Toronto, Ontario, M5S 1A7 Canada*

<sup>2</sup>*Department of Physics, Brookhaven National Laboratory, Upton, New York 11973, USA*

(Received 16 September 2004; published 16 March 2005)

Point-contact spectroscopy was performed on single crystals of the heavy-fermion superconductor CeCoIn<sub>5</sub> between 150 mK and 2.5 K. A pulsed measurement technique ensured minimal Joule heating over a wide voltage range. The spectra show Andreev-reflection characteristics with *multiple* structures which depend on junction impedance. Spectral analysis using the generalized Blonder-Tinkham-Klapwijk formalism for *d*-wave pairing revealed two *coexisting* order parameter components with amplitudes  $\Delta_1 = 0.95 \pm 0.15$  meV and  $\Delta_2 = 2.4 \pm 0.3$  meV, which evolve differently with temperature. Our observations indicate a highly unconventional pairing mechanism, possibly involving multiple bands.

DOI: 10.1103/PhysRevLett.94.107005

PACS numbers: 74.70.Tx, 74.20.Rp, 74.45.+c, 74.50.+r

The discovery of the heavy-fermion superconductor CeCoIn<sub>5</sub> has attracted widespread interest in the field of superconductivity [1]. Besides having the highest critical temperature  $T_c = 2.3$  K among heavy-fermion materials, CeCoIn<sub>5</sub> also shares some unconventional properties with the high- $T_c$  cuprates. First, CeCoIn<sub>5</sub> has shown pronounced non-Fermi-liquid behaviors, suggestive of quantum critical phenomena that could arise from competing orders [2,3]. Second, CeCoIn<sub>5</sub> has shown low-energy quasiparticle excitations and a power-law temperature dependence in the NMR spin relaxation, indicative of nodes in the superconducting energy gap [4–7]. These nodal characteristics are consistent with *d*-wave pairing symmetry [8], which could be produced by antiferromagnetic fluctuations [9]. Unlike the cuprates, on the other hand, CeCoIn<sub>5</sub> is an intermetallic compound with multiple sheets on the Fermi surface [10,11]. Such complex Fermi topology could involve several bands in the pairing process, giving rise to multiple pair potentials [12–14].

Point-contact spectroscopy (PCS) has been a proven microscopic technique for studying unconventional superconductors. For the high- $T_c$  cuprates, PCS provided the earliest measurements of the superconducting gap spectra [15]. In MgB<sub>2</sub>, PCS was key in revealing two coexisting *s*-wave gaps [16]. PCS has been previously performed on several heavy-fermion superconductors [17–21]. For superconductors with gap nodes, PCS can in general provide information on the pairing symmetry [22–25]. In this Letter, we report PCS measurements on single crystals of CeCoIn<sub>5</sub> in the temperature range 150 mK to 2.5 K. We observed Andreev-reflection characteristics with multiple structures, whose dependence on junction impedance indicates two *coexisting* order parameter components (OP) with nodal characteristics. These OP's show sizable amplitudes relative to  $T_c$  and different evolutions with temperature. Our observations suggest a highly unconventional pairing mechanism, possibly involving multiple bands.

In PCS, electronic transmission between a normal metal and a superconductor is measured as conductance  $dI/dV$  versus bias voltage  $V$  across a ballistic contact junction. For a transparent contact,  $dI/dV$  is primarily determined by Andreev reflection, based on the conversion of electrons or holes into Cooper pairs, which doubles  $dI/dV$  inside the superconducting energy gap. For nontransparent junctions,  $dI/dV$  involves both Andreev reflection and quasiparticle tunneling. The standard model for calculating  $dI/dV$  was given by the Blonder-Tinkham-Klapwijk (BTK) theory for *s*-wave pairing [26] and subsequently generalized for *d*-wave pairing [27,28]. A key spectral signature of the *d*-wave gap nodes is the zero-bias conductance peak, which arises from *surface* states bound by phase interference between consecutively Andreev-reflected quasiparticles [29]. This peak structure is to be distinguished from the hump structure associated with conventional Andreev *bulk* states. In the generalized BTK scenario, relative manifestation of the Andreev surface versus bulk states depends on both junction orientation and a dimensionless parameter  $Z$  representing junction impedance [30], thus allowing the OP to be studied [23,28].

The single crystals of CeCoIn<sub>5</sub> used in this work were grown by a self-flux method [1], and characterized by both x-ray diffraction and magnetic susceptibility to confirm material uniformity. The crystals were platelets approximately  $1 \times 1 \times 0.2$  mm<sup>3</sup> in size, each showing a sharp superconducting transition at  $T_c = 2.3$  K. The crystal surfaces were etched with HCl and rinsed with ethanol prior to measurement in order to remove any residual In flux. High purity Pt-Ir tips were used as normal-metal electrodes, gently pressed onto the *c*-axis face of each crystal with a spring-cushioned differential micrometer. This point-contact mechanism was attached to the mixing chamber of a high cooling-power <sup>3</sup>He/<sup>4</sup>He dilution refrigerator, and enabled the junction impedance to be varied *in situ* at low temperatures. The point contacts we measured were in the

0.2–1  $\Omega$  range, consistent with the contact size being in the ballistic regime [31]. To minimize Joule heating in the junction over a wide voltage range, our spectroscopy data were acquired by a pulsed technique: 2 ms current pulses were applied through the contact in 20% duty cycles, and the junction voltage was measured 80 times within each pulse and then averaged. The  $I$  vs  $V$  curves were obtained by varying the current level, and then numerically differentiated to obtain the  $dI/dV$  vs  $V$  spectra.

Two types of spectra were observed in our measurements, depending on the point-contact impedance. These measurements were reproducible on multiple spots over different samples and repeated at each spot to rule out any surface destruction by the point contact. Figure 1 shows  $dI/dV$  spectra taken at 0.43 K well below  $T_c$  after normalization relative to spectra taken above  $T_c$ . The top panel is for a 0.4  $\Omega$  junction, and the bottom panel is for a 0.2  $\Omega$  junction. Distinct spectral features are seen in the top panel, with a sharp zero-bias peak dipping at  $\sim \pm 1$  mV into a broad spectral hump  $\sim \pm 2.5$  mV in width. Small kinks are also visible on the peak at  $\sim \pm 0.3$  and  $\sim \pm 0.5$  mV. The main peak, dip, and hump structures evolve differently with decreasing junction impedance. As seen in the bottom panel, the peak becomes an asymmetric inner hump  $\sim \pm 1$  mV in width, the dips get filled in, while the outer hump remains largely unchanged. These hump structures are the classic signatures of Andreev reflection, which introduces excess spectral states inside the energy gap [26]. These excess states expectedly diminish with temperature, as is evident in the 1.5 K data [dashed curve in Fig. 1(b)]. The zero-bias peak, on the other hand, is key evidence for nodes in the gap [27]. It is worth noting

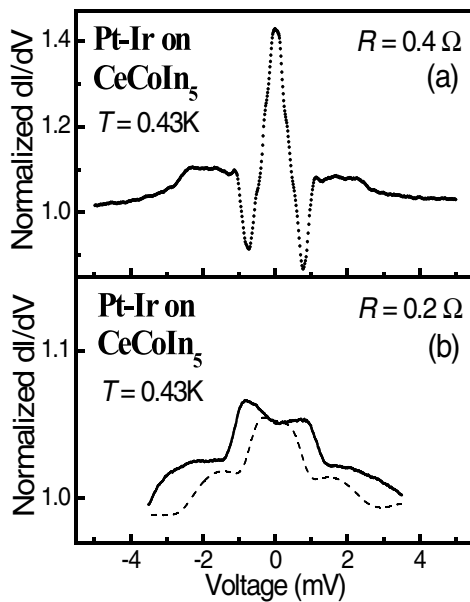


FIG. 1. Normalized  $dI/dV$  vs  $V$  data for Pt-Ir point contacts on CeCoIn<sub>5</sub> at 0.43 K. Top panel (a) is for a 0.4  $\Omega$  junction. Bottom panel (b) is for a 0.2  $\Omega$  junction, with the 1.5 K curve (dashed) also plotted to clearly show the double humps.

that peak and hump structures of similar shapes and energy scales have been reported in an earlier PCS study of CeCoIn<sub>5</sub>, although appearing separately in different spectra [32]. Our measured spectra are clearly hybrid in character, each containing multiple structures.

To identify the multiple spectral features observed in our data, we consider theoretical spectra from the generalized BTK model. Shown in the top panels of Fig. 2 are the simulated  $dI/dV$  spectra for a  $d$ -wave OP, plotted in normalized units vs  $eV/\Delta$ , where  $\Delta$  is the  $d$ -wave gap maximum [33]. The choice of  $d$ -wave symmetry here is motivated by both thermodynamic and transport data [6,7], and is intended to illustrate the generic spectral dependence on junction orientation and impedance. The curves in Fig. 2(a) are for a high-impedance ( $Z = 1$ ) junction, and the curves in Fig. 2(b) are for a low-impedance ( $Z = 0.5$ ) junction. In each plot, the dotted/solid curve is for a nodal/antinodal junction (normal to a nodal/antinodal axis), while the dashed curve models the effect of junction roughness by averaging over all intermediate orientations. Note that an ideal  $c$ -axis junction would produce similar spectra as the antinodal case, since there is no OP sign change about the junction normal in either case to allow for Andreev interference. The overall spectral evolution between peak and hump structures is a direct manifestation of the competition between Andreev surface and bulk states [27].

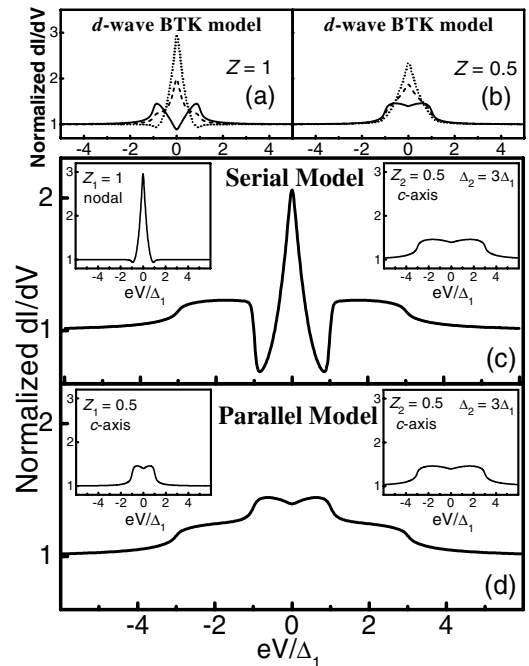


FIG. 2. Spectral simulations using the generalized  $d$ -wave BTK formalism. (a) and (b) are for  $Z = 1$  and  $Z = 0.5$  junctions, with nodal (dotted curves), antinodal or  $c$ -axis (solid curves), and angle-averaged (dashed curves) orientations. (c) and (d) show serial and parallel superpositions of two spectral contributions (insets) for two OP's with  $\Delta_2 = 3\Delta_1$  and different  $Z$ 's.

From these generic spectral simulations, the data in Fig. 1 can be interpreted as the *superposition* of two types of spectral contributions. Namely, the sharp peak structure comes from Andreev surface states due to a high- $Z$  nodal junction, and the broad hump structures come from Andreev bulk states due to low- $Z$  antinodal junctions. The appearance of two effective  $Z$ 's, with very different dependences on junction impedance, is indicative of different Andreev coupling to two distinct OP's. To demonstrate this two-OP scenario, we have developed a superposition model, based on the "serial" precedence of surface over bulk states in junction transmission. More specifically, when bulk spectra from two different OP's coexist, their superposition is essentially *additive* [16], since bulk states can be accessed in "parallel." However, when *both* surface and bulk spectra are involved, the junction transmission becomes effectively "serial," thus justifying a *multiplicative* superposition within energies ( $|eV| < \Delta$ ) where Andreev surface states can readily form. This serial model is demonstrated in Fig. 2(c), by superposing a peak spectrum (left inset) with a hump spectrum (right inset) of triple the energy scale (i.e.,  $\Delta_2 = 3\Delta_1$ ). Here the component spectra were multiplied for  $|eV| < \Delta_1$  and added for  $|eV| > \Delta_1$ , following our model justifications. The peak-dip-hump structures seen in the data of Fig. 1(a) are remarkably well reproduced here in Fig. 2(c). For comparison, the parallel model superposing two low- $Z$  bulk spectra (insets) is shown in Fig. 2(d), also generically reproducing the multiple-hump data seen in Fig. 1(b). The overall spectral resemblance between our simulations and data is robust evidence for the coexistence of two OP's.

Some general remarks about our two-OP spectral analysis should be made. First, our model was intended to show generically how two coexisting OP's with gap nodes could produce the multiple spectral structures observed. The distinctively serial relationship between the peak and hump structures clearly establishes the surface-state nature of the former, as arising from Andreev interference for a nodal OP. However, although our data can be explained within a  $d$ -wave framework, we cannot rule out the presence of other OP line or point nodes, along either the pole or the equator, such as in the case of  $\text{UPt}_3$  [34]. Precise determination of the pairing symmetry in  $\text{CeCoIn}_5$  would require a systematic study of the spectral anisotropy [23], along with an extension of the generalized BTK theory beyond its two-dimensional formulation. Second, the non-trivial spectral evolution we observed versus junction impedance indicates a complex  $k$ -space dependence of  $Z$ , with the nodal-junction states dominating at high  $Z$  and antinodal-junction states dominating at low  $Z$ . While roughness could allow for nodal-junction surfaces to exist on a nominally  $c$ -axis crystal, a detailed explanation of the peak-to-hump evolution would require full understanding of how  $Z$  depends on the complex band structure of  $\text{CeCoIn}_5$  [30]. For example, multiband coupling could in theory affect the formation of Andreev surface states [35]. The effects of band structure on quasiparticle tunneling

have also been studied [36]. Third, the spectral heights tend to be smaller in the data than in the model, a difference which could be attributed to nonsuperconducting spectral contributions from either uncondensed quasiparticles [37] or Kondo scattering [38].

The temperature dependence of our spectral data was also examined. Figure 3 shows spectral evolution of the data from Fig. 1 in the temperature range 150 mK to 2.5 K. The spectra are staggered for clarity, with arrows in Fig. 3(a) to indicate the two-OP amplitudes determined from the serial model above, and a dotted baseline in Fig. 3(b) to underscore the "excess" spectral area associated with bulk Andreev states. The OP amplitudes  $\Delta_1(T)$  and  $\Delta_2(T)$  are plotted in Fig. 3(c), along with theoretical (dotted) curves calculated from the BCS gap equation. The excess spectral area  $S$  is similarly plotted in Fig. 3(d), after normalization by its base-temperature value  $S_0$  [19]. From Fig. 3(c), it is clear that both OP amplitudes approach distinct zero-temperature values,  $\Delta_1 = 0.95 \pm 0.15$  meV and  $\Delta_2 = 2.4 \pm 0.3$  meV, and vanish near  $T_c = 2.3$  K, consistent with both components being of the same superconducting order. This common  $T_c$  also argues against the presence of a proximity-induced superconducting layer in our junctions, which should cause the smaller order parameter component to vanish below the bulk  $T_c$  [16]. However, while  $\Delta_1(T)$  is well described by the BCS gap equation,  $\Delta_2(T)$  deviates markedly from mean-field behavior.

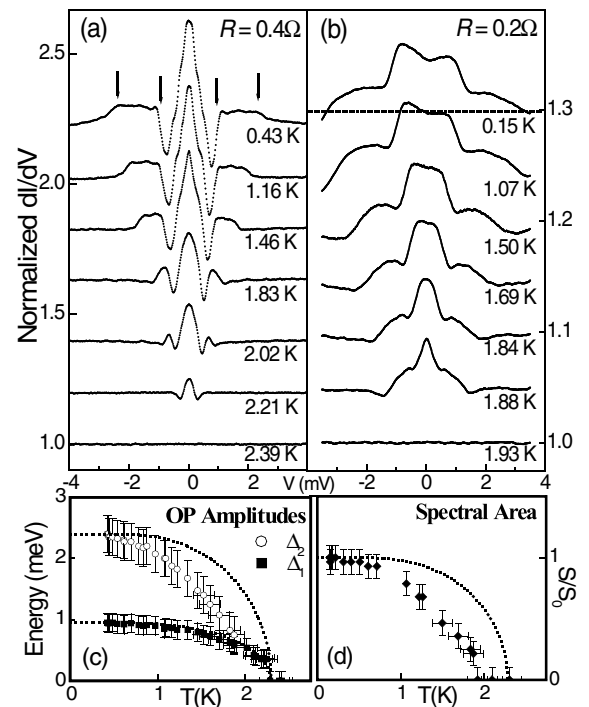


FIG. 3. Temperature dependence of the data from Fig. 1. A subset of the spectral evolutions are shown in (a) and (b). The OP amplitudes  $\Delta_1(T)$  and  $\Delta_2(T)$  determined from (a) are plotted in (c). The reduced spectral area  $S/S_0$  extracted from (b) is plotted in (d). Theoretical BCS curves (dotted) are included to indicate deviations from mean-field behavior.

ior. This deviation is also evident in the reduced spectral area ( $S/S_0$ ) plot in Fig. 3(d), indicating a predominance of the larger OP for parallel superposition. Similar deviations have been observed in other heavy-fermion superconductors, and attributed to the nodality of highly complex pairing symmetries [19–21]. Alternatively, the difference between  $\Delta_1(T)$  and  $\Delta_2(T)$  could be the signature of novel interplay between two different types of order [39,40].

Finally we discuss the physical implications of our results on the pairing mechanism in CeCoIn<sub>5</sub>. First, assuming that each of the two energy scales identified above can be directly assigned to a superconducting OP, they would correspond to gap-to- $T_c$  ratios of  $2\Delta_1/k_B T_c = 9.5 \pm 1.5$  and  $2\Delta_2/k_B T_c = 24 \pm 3$ . These ratios are much larger than the BCS weak-coupling value of 3.5 for phonon-mediated pairing, and well beyond the strong-coupling limit even after  $d$ -wave corrections [41]. One conceivable way to enhance the gap-to- $T_c$  ratio is through interband coupling, whereby carriers from different bands could interact to result in multiple pair potentials sharing a common  $T_c$  [12]. This multiband scenario would be physically plausible for CeCoIn<sub>5</sub>, considering that its Fermi surface has four distinct sheets with different topologies and effective masses [10,11]. Furthermore, Andreev scattering for a heavy-mass 2D sheet would be inherently weaker than for a light-mass 3D sheet, due to poorer Fermi-velocity matching across the junction [30]. This multiband effect could provide a natural explanation for the two different  $Z$  scales observed in our spectra. However, even allowing for interband coupling between highly disparate densities of states [12], a sizable “intrinsic”  $2\Delta/k_B T_c$ , intermediate between  $\approx 9.5$  and 24, may still be needed to explain our data [12,42]. Such an intrinsically large gap-to- $T_c$  ratio would present a serious challenge to current theoretical formulations [41,43], at least within the Fermi-liquid framework, thus indicating a highly unconventional pairing mechanism in CeCoIn<sub>5</sub>.

In summary, we have performed point-contact spectroscopy on the heavy-fermion superconductor CeCoIn<sub>5</sub>. Andreev-reflection characteristics with multiple structures were observed. Spectral analysis using the generalized BTK formalism revealed two coexisting order parameter components with nodal symmetry and sizable amplitudes. These observations suggest a highly unconventional pairing mechanism in a multiband scenario.

Work supported by: NSERC, CFI/OIT, Canadian Inst. for Advanced Research; Division of Materials Sciences, Office of Basic Energy Sciences, and US Dept. of Energy under Contract No. DE-AC02-98CH10886.

\* Permanent address: Inst. Surface Chemistry, N.A.S. Ukraine, Kyiv, Ukraine.

- [1] C. Petrovic *et al.*, J. Phys. Condens. Matter **13**, L337 (2001).
- [2] V. A. Sidorov *et al.*, Phys. Rev. Lett. **89**, 157004 (2002).
- [3] J. Paglione *et al.*, Phys. Rev. Lett. **91**, 246405 (2003).
- [4] R. Movshovich *et al.*, Phys. Rev. Lett. **86**, 5152 (2001).
- [5] Y. Kohori *et al.*, Phys. Rev. B **64**, 134526 (2001).
- [6] K. Izawa *et al.*, Phys. Rev. Lett. **87**, 057002 (2001).
- [7] H. Aoki *et al.*, J. Phys. Condens. Matter **16**, L13 (2004).
- [8] C. C. Tsuei and J. R. Kirtley, Rev. Mod. Phys. **72**, 969 (2000); D. van Harlingen, Rev. Mod. Phys. **67**, 515 (1995).
- [9] P. Monthoux and G. Lonzarich, Phys. Rev. B **66**, 224504 (2002), and references therein.
- [10] T. Maehira *et al.*, J. Phys. Soc. Jpn. **72**, 854 (2003).
- [11] D. Hall *et al.*, Phys. Rev. B **64**, 212508 (2001); R. Settai *et al.*, J. Phys. Condens. Matter **13**, L627 (2001).
- [12] H. Suhl *et al.*, Phys. Rev. Lett. **3**, 552 (1959).
- [13] A. Y. Liu *et al.*, Phys. Rev. Lett. **87**, 087005 (2001).
- [14] P. Canfield and G. Crabtree, Phys. Today **56**, No. 3, 34 (2003).
- [15] J. Zasadzinski, in *The Physics of Superconductors*, edited by K. H. Bennemann (Springer, New York, 2003).
- [16] P. Szabo *et al.*, Phys. Rev. Lett. **87**, 137005 (2001).
- [17] A. Nowack *et al.*, Phys. Rev. B **36**, 2436 (1987).
- [18] K. Hasselbach *et al.*, Phys. Rev. B **46**, 5826 (1992).
- [19] Y. DeWilde *et al.*, Phys. Rev. Lett. **72**, 2278 (1994).
- [20] For a recent review, see Y. Naidyuk *et al.*, J. Phys. Condens. Matter **10**, 8905 (1998).
- [21] C. Walti *et al.*, Phys. Rev. Lett. **84**, 5616 (2000).
- [22] L. Alff *et al.*, Phys. Rev. B **55**, R14757 (1997).
- [23] J. Y. T. Wei *et al.*, Phys. Rev. Lett. **81**, 2542 (1998).
- [24] Z. Mao *et al.*, Phys. Rev. Lett. **87**, 037003 (2001).
- [25] A. Biswas *et al.*, Phys. Rev. Lett. **88**, 207004 (2002).
- [26] G. E. Blonder *et al.*, Phys. Rev. B **25**, 4515 (1982).
- [27] C.-R. Hu, Phys. Rev. Lett. **72**, 1526 (1994).
- [28] Y. Tanaka *et al.*, Phys. Rev. Lett. **74**, 3451 (1995).
- [29] M. Aprili *et al.*, Phys. Rev. Lett. **83**, 4630 (1999).
- [30] The BTK parameter  $Z$  also has implicit dependence on the junction Fermi-velocity matching and thus on the superconductor’s bare band structure. See, e.g., G. Deutscher and P. Nozieres, Phys. Rev. B **50**, 13557 (1994).
- [31] Using the Sharvin formula for the contact resistance  $R = 4\rho l/3\pi a^2$ , with  $\rho \sim 3 \mu\Omega \text{ cm}$  [1] and  $l \sim 80 \text{ nm}$  at  $T_c$  [4] for CeCoIn<sub>5</sub>, we estimate our contact radius  $a < 70 \text{ nm}$ , satisfying the ballistic criterion  $a < l$  [26]. This criterion would be further justified if a lower-temperature  $\rho \sim 0.3 \mu\Omega \text{ cm}$  [3] were used, giving  $l \sim 800 \text{ nm}$ .
- [32] G. Goll *et al.*, Acta Phys. Pol. B **34**, 575 (2003).
- [33] In our simulations, temperature was fixed at  $k_B T = 0.03\Delta$ , consistent with experimental conditions.
- [34] R. Joynt and L. Taillefer, Rev. Mod. Phys. **74**, 235 (2002).
- [35] K. Voelker and M. Sigrist, cond-mat/0208367.
- [36] J. Y. T. Wei *et al.*, Phys. Rev. B **57**, 3650 (1998).
- [37] D. F. Agterberg *et al.*, Phys. Rev. Lett. **78**, 3374 (1997).
- [38] Z. Fisk *et al.*, Science **239**, 33 (1988).
- [39] N. D. Mathur *et al.*, Nature (London) **394**, 39 (1998).
- [40] E. Demler *et al.*, Phys. Rev. Lett. **87**, 067202 (2001).
- [41] E. J. Nicol and J. P. Carbotte, Phys. Rev. B **71**, 054501 (2005).
- [42] M. Iavarone *et al.*, Phys. Rev. Lett. **89**, 187002 (2002).
- [43] Y. Bang and A. V. Balatsky, Phys. Rev. B **69**, 212504 (2004).